Adsorption 11: 307–312, 2005

Impact of Potential Models on Adsorption of Linear Molecules on Carbon Black

D.D. DO* AND H.D. DO
Department of Chemical Engineering, University of Queensland, St Lucia, QLD 4072, Australia
duongd@cheque.uq.edu.au

Abstract. In this paper, we investigate the effects of potential models on the description of equilibria of linear molecules (ethylene and ethane) adsorption on graphitized thermal carbon black. GCMC simulation is used as a tool to give adsorption isotherms, isosteric heat of adsorption and the microscopic configurations of these molecules. At the heart of the GCMC are the potential models, describing fluid-fluid interaction and solid-fluid interaction. Here we studied the two potential models recently proposed in the literature, the UA-TraPPE and AUA4. Their impact in the description of adsorption behavior of pure components will be discussed. Mixtures of these components with nitrogen and argon are also studied. Nitrogen is modeled a two-site plus discrete charges while argon as a spherical particle. GCMC simulation is also used for generating simulation mixture isotherms. It is found that co-operation between species occurs when the surface is fractionally covered while competition is important when surface is fully loaded.

Keywords: adsorption, Monte Carlo, ethylene, ethane, graphitized thermal carbon black

Introduction

Monte Carlo simulation, molecular dynamics simulation (MD) and density functional theory have been increasingly applied to solve physical problems, including adsorption problems. Complex molecules and highly ordered surfaces can be readily accounted for by the MC and MD methods. The good description of experimental data by these molecular methods, however, critically depends on the potential models that correctly describe the fluid-fluid interaction and the solid-fluid interaction. In this paper, we consider linear molecules, ethylene and ethane, and investigate the two recently proposed potential models. One model is the UA-TrapPPE model, whose molecular parameters are given by Martin and Siepmann (1998) for ethane and Wick et al. (2000) for ethylene. The other model is the AUA4 model, of which the molecular parameters are provided by Ungerer et al. (2000) and Bourasseau et al. (2003). These parameters were obtained by matching the simulation results against the vapor-liquid equilibria data. We will compare the performance of these models on their ability to describe the adsorption isotherms on graphitized thermal carbon black and the isosteric heat versus loading. Graphitized thermal carbon black has been used as a reference material for characterizing activated carbon (Kruk et al., 1999), and adsorption data of many substances are available in the literature (Avgul and Kiselev, 1970).

*To whom correspondence should be addressed.

Model

Ethylene and ethane are treated as a particle composed of 2 united atoms. The site-site interaction is described by the 12-6 Lennard-Jones potential equation. The interaction potential energy of a site a on a molecule i and a site b on a molecule j is given by:

$$\varphi_{i,j}^{(a,b)} = 4\varepsilon^{(a,b)}\left[\left(\frac{\sigma^{(a,b)}}{r_{i,j}^{(a,b)}}\right)^{12} - \left(\frac{\sigma^{(a,b)}}{r_{i,j}^{(a,b)}}\right)^{6}\right] \quad (1)$$

where the subscript denotes for molecule while the upperscript for interaction site. Each interaction site is characterized by two parameters. Given the site-site interaction energy, the molecule-molecule interaction energy is then obtained by summing interactions of all sites of the two molecules. In GCMC of a simulation box, the calculation of dispersive interaction energy is carried out with the usual minimum image convention.

For nitrogen, it is modeled as two dispersive sites (on nitrogen atom centers) and a set of charges to account for the quadrupole and higher moments (the quadrupole moment of nitrogen is -4.9×10^{-40} Cm^{-2}). The dispersive interaction is calculated as in Eq. (1). The electrostatic interaction is calculated via the Coulomb law, of which the interaction between a charge "α" on a molecule "i" and a charge "β" on a molecule "j" is determined from:

$$\varphi_{q;i,j}^{(\alpha,\beta)} = \frac{1}{4\pi\varepsilon_0} \cdot \frac{q_i^{\alpha} q_j^{\beta}}{r_{i,j}^{(\alpha,\beta)}} \tag{2}$$

where ε_0 is the permittivity of free space ($\varepsilon_0 = 8.8543 \times 10^{-12}$ C^{2}J^{-1}m^{-1}), The molecular parameters and the set of discrete charges for nitrogen are taken from Murthy (1983). The calculation of electrostatic interaction energy is done directly for charges and their images, and the long range correction of Heyes and van Swol (1981) is used.

The solid-fluid interaction is determined by assuming the surface is homogeneous, and the Steele equation can used for this purpose. In the GCMC simulations of adsorption on graphitized thermal carbon black and in slit pores we use the following parameters. The box length is equal to 10 times the collision diameter, and the cut-off radius is taken to be half of the box length. The number of cycle in the equilibration step and in the collecting statistics step is 50,000 each, and in each cycle we have N displacements and rotations (N is the number of particles) and the number of attempts to exchange particle with the surrounding is chosen such that the acceptance rate is 2%. For simulations of an open graphitized thermal carbon black surface, we use a slit pore having width of 80 A. This width is large enough for that slit pore to mimic two independent surfaces. In presenting the GCMC simulation results we plot them as (i) average surface excess (for open surface) and average pore density (for slit pore) versus pressure, (ii) 2D-plot of local density versus the distance from the pore surface, and (iii) 3D-plot of local density versus the distance from the pore surface and the angle θ formed between the molecular axis and the z-direction.

The utility of the GCMC simulations is not only in the generation of adsorption isotherm and the microscopic configuration of molecules, but also in the calculation of various thermodynamics quantities, for example the isosteric heat. Using the fluctuation theory, the isosteric heat is calculated from (Nicholson and Parsonage, 1982):

$$q_{\text{iso}} = \frac{\langle U\rangle\langle N\rangle - \langle U\,N\rangle}{\langle N^2\rangle - \langle N\rangle\langle N\rangle} + k_B T$$

where N is the number of particle and U is the configuration energy of the system.

Discussion

First we present in Fig. 1 the results of adsorption of ethylene and ethane on graphitized carbon black at 175 K. The solid lines are the results from the GCMC

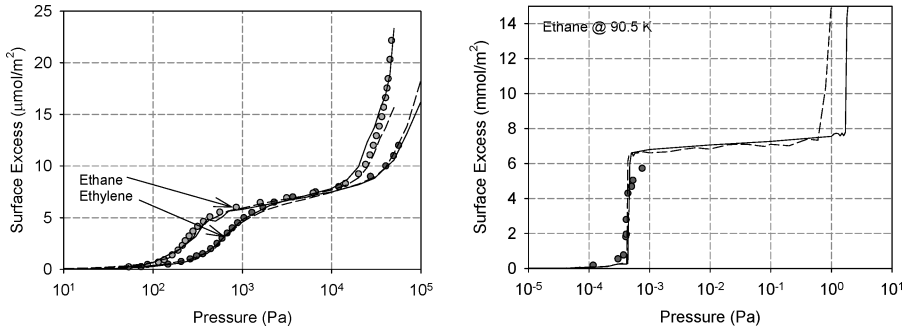

Figure 1. (a) Adsorption isotherms of ethylene and ethane at 175 K (b) Adsorption isotherm of ethane at 90.5 K; (solid line: UA-TraPPE model; dashed line: AUA4 model; symbols: Experimental data).

simulations using the UA-TraPPE model, while the dashed lines for the AUA4 model. The experimental data are available from Avgul and Kiselev (1970) and presented as symbols in this figure. Both models describe reasonably well the adsorption data, and for the case of ethane the description is good up to the three layers adsorbed on the surface. The good description by both models is also observed for 183, 193, 203 and 213 K, at which data are available in the literature (Avgul and Kiselev, 1970). Observation of these isotherms shows that there are no 2D condensation on the surface, and this is due to the fact that these temperatures are not low enough for it to occur. To check this, we use the low temperature data of ethane (Graham, 1958). At this low temperature of 90.5 K (which is the triple point of ethane), limited data obtained by Graham does show 2D transition. We test this with the UA-TraPPE and AUA4 model, and the results are shown in Fig. 1(b) together with the experimental data. The good description of this 2D condensation by these models with the GCMC method highlights the potential of the MC method as a useful tool to study adsorption equilibria.

Having seen the 2D transition at 90.5 K, the 2D-critical temperature of ethylene and ethane must be between 90.5 and 175 K. To search for this, we perform a series of GCMC simulations for these two species for a number of temperatures. Some of these results are shown in Fig. 2 for the UA-TraPPE model. From these plots, we can estimate the 2D-critical temperatures for ethylene and ethane to be 110 and 125 K, respectively. These values are in good agreement with 109 and 130 K, reported by Steele (1996). The values obtained with the AUA4 model are slightly smaller than those predicted by the UA-TraPPE model.

Having studied the isotherms and the derived 2D-critical temperature, we now study the behavior of isosteric heat of adsorption versus loading. Data for heat of adsorption for ethylene and ethane were reported by Avgul and Kiselev (1970). We show in Fig. 3 the results of isosteric heat obtained from the GCMC simulation for ethylene (3a) and ethane (3b), using the UA-TraPPE

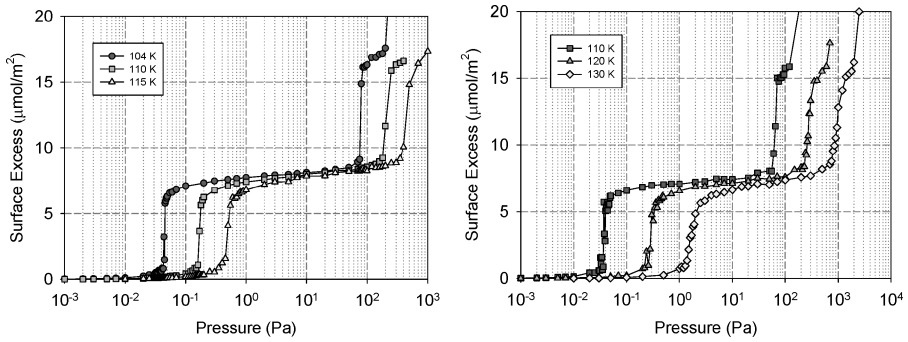

Figure 2. Isotherms of (a) ethylene and (b) ethane at various temperatures obtained from GCMC simulation using UA model.

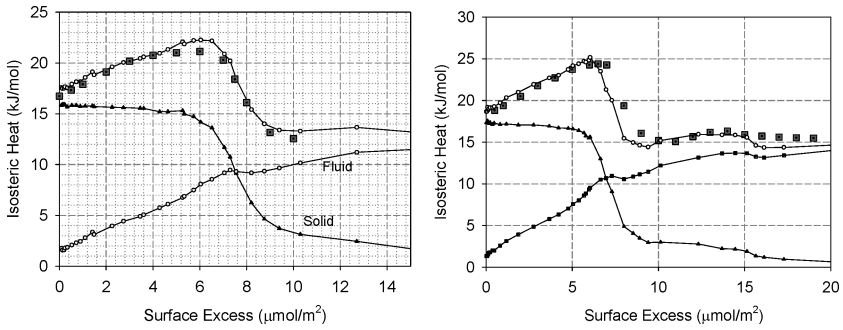

Figure 3. Isosteric heat of (a) ethylene at 173 K and (b) ethane at 158 K versus loading (Top curve: Isosteric heat; Fluid: contribution from fluid-fluid interaction; Solid: contribution from solid-fluid interaction; Square symbols: Experimental data).

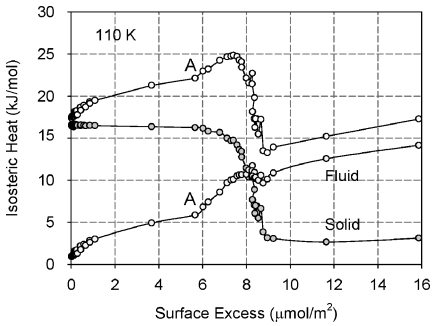

Figure 4. Isosteric heat of ethylene on carbon black surface at 110 K and contributions from solid-fluid and fluid-fluid interaction (see Fig. 3 for explanation of different curves).

model. The agreement between the simulation results and the data is quite excellent. The AUA4 slightly over-predicts the heat of adsorption (not shown). It is worthwhile to simulate the isosteric heat at 2D-critical temperature. This is shown in Fig. 4 for ethylene at 110 K. Plotted in this figure are the isosteric heat versus surface excess and the separate contributions from fluid-fluid and solid-fluid interactions. We see that the heat from fluid-fluid interaction shows a kink at A (Fig. 4), and this is due to the 2D-transition in the adsorption isotherm. This kink is then observed in the total isosteric heat, and hence it could be used as an indicator for the 2D-condensation on surface. The heat contributed by the solid-fluid shows a small decline in the region of monolayer coverage (surface loadings less than 7 μmol/m^2) and then a sharp decline when second layer is formed. The small decrease in the solid-fluid interaction is due to the vertical orientation of molecules in the first layer, which is resulted from the two factors. One is entropic factor, which favors random orientation, and the other is due to the energetic factor resulted from their interactions with molecules in the second layer.

The orientation of molecules in various layers is determined from the plots of 2D- and 3D-density distribution versus distance from the surface and also the angle formed between the molecular axis and the z-coordinate. We show typical plots for ethylene using the UA-TraPPE model at $P = 100{,}000$ Pa and $T = 173$ K (Fig. 5).

There is no surprise that the first peak (first layer) is sharper than the second one. This is a direct result of the strong solid-fluid interaction on the first layer. Also because of this solid interaction, most ethylene molecules in the first layer adopt parallel orientation while some adopting vertical orientation. The latter is due to the fluid-fluid interaction between them and the molecules in the second layer. The second layer, on the other hand, has weaker solid-fluid interaction; hence molecules in this layer do not have any preferential orientation.

Having seen the potential of the GCMC as a tool to investigate adsorption, we now turn to mixture adsorption and study the mixtures- ethylene/argon, ethylene/nitrogen, ethylene/ethane—in slit pores of various sizes. For illustration, we show a typical result of adsorption of ethylene/argon mixture in 10 A slit pore and $T = 200$ K in Fig. 6(a) (using UA-TraPPE model). At this temperature, ethylene is a sub-critical fluid while argon is a super-critical fluid. In this plot, we plot the average pore density of ethylene versus its partial pressure as solid line. The partial pressure of argon is maintained constant at 100,000 Pa. For comparison, we also plot in the same figure the adsorption of pure ethylene versus pressure (dashed line).

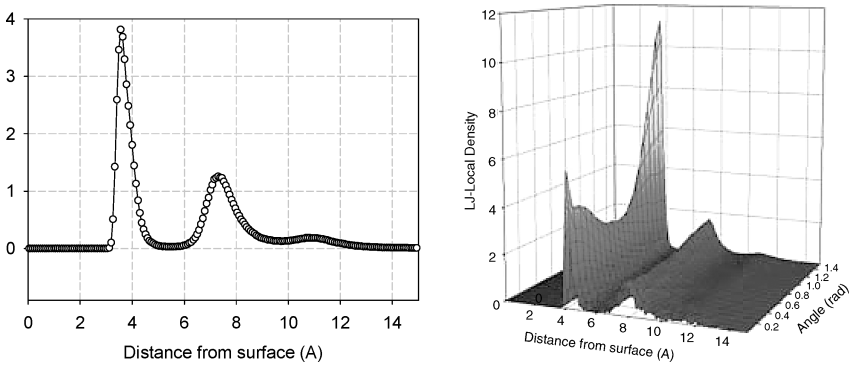

Figure 5. Local density distribution of ethylene at 173 K and 100,000 Pa, obtained from UA-TraPPE (a) 2D-plot versus distance (b) 3D-plot versus distance and angle θ.

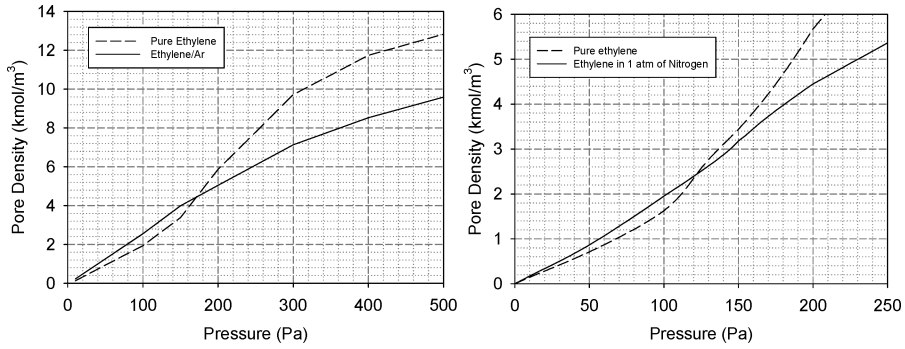

Figure 6. Pore Density of ethylene vs partial pressure of ethylene (a) in ethylene/argon mixture (b) in ethylene/nitrogen mixture for 10 A slit pore and $T = 200$ K.

In the low pressure region (less than 170 Pa), the amount of ethylene adsorbed in the case of mixture is greater than the case of pure ethylene, while the opposite is true in the higher pressure region. The latter is a typical example of competition, and the former is the so-called *co-operative* adsorption. The co-operative adsorption is possible when the surface is only fractionally covered, and as such there is no issue of competition among different species for adsorption space. In this case of ethylene and argon, the presence of argon molecules on the surface actually exerts interaction with ethylene and it is this interaction that enhances the amount of ethylene adsorbed. However, when the surface is fully loaded the competition among different species is an important issue to consider. Because of this competition, the amount of ethylene adsorbed in the case of mixture is now less than that for the case of pure ethylene. The phenomenon of *co-operation* and *competition* occurs for all mixtures, and this can be further illustrated with the mixture of ethylene and nitrogen in Fig. 6(b). Although not shown here, the same conclusion is derived for ethylene/ethane mixture.

To illustrate further the co-operative and competitive adsorption, we study the adsorption of ethylene and argon mixture in 15A slit pore at 200 K. As expected, at low pressures the co-operation occurs but the effect is not as strong as in smaller pores, due to the weaker solid-fluid interaction in large pores. For high pressures, competition occurs, but a question is raised about argon adsorption. We show in Fig. 7(a), the LJ-local density distribution ($\rho\sigma^3$) of argon in 15 A for two cases. In the first case, we have argon and ethylene in the mixture, and their respective partial pressures are 100,000 and 10,000 Pa. While in the second case, we have pure argon of 100,000 Pa. It is seen in this figure that in the case of pure argon (dashed line), the amount of argon adsorbed is about 19 kmol/m^3; however, in the case of mixture of argon and ethylene, the amount of argon adsorbed is 11.7 kmol/m^3 (solid line).

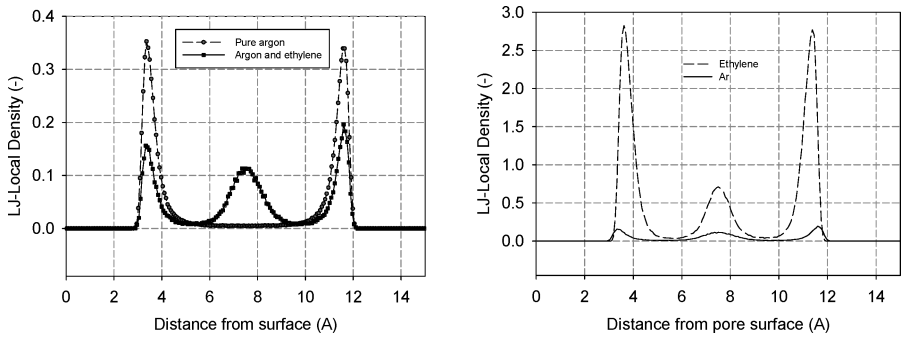

Figure 7. (a) 2D-density distribution of argon in mixture of argon/ethylene (solid line) and pure argon (dashed line); (b) 2D-density distribution of argon (solid line) and ethylene (dashed line) in argon/ethylene mixture.

Even though the argon adsorbed amount in the case of pure fluid is greater, the amount of 11.7 kmol/m^3 is quite significant in the case of mixture in the light that ethylene is a stronger adsorbing species and as such it dominates argon in all layers as seen in Fig. 7(b). Since argon in the case of mixture can not compete with ethylene in the contact layers, it must adsorb in the inner core (the middle peak in Fig. 7(a)) and that is made possible due to the interaction between the argon and ethylene molecules.

Conclusion

GCMC simulation has been demonstrated in this paper as a useful tool to study adsorption isotherms, isosteric heat of adsorption, microscopic configuration of adsorbed molecules and the detailed picture of how different species interact inside the confined space of slit pores. Co-operative and competitive adsorption are possible for mixture, with the former occurring when surface is fractionally covered and the latter for fully covered surface. Of the two potential models studied, the UA-TraPPE model performs slightly better than the AUA4 model.

Acknowledgments

Support from the Australian Research Council is gratefully acknowledged.

References

Avgul, N.N. and A.V. Kiselev, "Physical Adsorption of Gases and Vapors on Graphitized Carbon Blacks," *Chemistry and Physics of Carbon*, **6**, 1–124 (1970).

Bourasseau, E., M. Haboudou, A. Boutin, A. Fuchs, and P. Ungerer, "New Optimization Method for Intermolecular Potentials," *J. Chem. Phys*., **118**, 3020–3034 (2003).

Graham, D., "The Effects of Small Degrees of Adsorbent Heterogeneity on Two-Dimensional Condensation in Adsorbed Monolayer," *J. Phys. Chem*., **62**, 1210–1211 (1958).

Heyes, D.M. and F. van Swol, "The Electrostatic Potential and Field in the Surface Region of Lamina and Semi-Infinite Point Charge Lattice," *J. Chem. Phys*., **75**, 5051–5058 (1981).

Kruk, M., Z. Li, M. Jaroniec, and W.R. Betz, "Nitrogen Adsorption Study of Surface Properties of Graphitized Carbon Blacks," *Langmuir*, **15**, 1435–1441 (1999).

Martin, M. and J. Siepmann, "Transferrable Potentials for Phase Equilibria," *J. Phys. Chem*., **102**, 2569–2577 (1998).

Murthy, C.S., S.F. O-Shea, and I.R. McDonald, "Electrostatic Interactions in Molecular Crystals. Lattice Dynamics of Solid Nitrogen and Carbon Dioxide," *Mol. Phys*., **50**, 531–541 (1983).

Nicholson, D. and N.G. Parsonage, *Statistical Mechanics of Adsorption*, Academic Press, London, 1982.

Steele, W.A. "Monolayers of Linear Molecules Adsorbed on the Graphite Basal Plane," *Langmuir*, **12**, 145 (1996).

Ungerer, P., C. Beauvais, J. Delhommelle, A. Boutin, B. Rousseau, and A. Fuchs, "Optimization of the Anisotropic United Atoms Intermolecular Potential for *n*-Alkanes," *J. Chem. Phys*., **112**, 5499–5510 (2000).

Wick, C.D., M. Martin, and J. Siepmann, "Transferable Potentials for Phase Equilibria. 4. United-Atom Description of Linear and Branched Alkenes and Alkylbenzenes," *J. Phys. Chem. B*, **104**, 8008–8016 (2000).